Numerical modelling of historical masonry structures with the finite element code NOSA-ITACA

M. Girardi, C. Padovani, D. Pellegrini, M. Porcelli, L. Robol

Abstract This chapter presents the finite element code NOSA-ITACA for static and modal analyses of masonry structures of architectural interest. NOSA-ITACA adopts the constitutive equation of masonry-like materials, which considers masonry a non-linear elastic material with zero tensile strength. The capability of modelling restoration and consolidation operations makes the code a helpful tool for maintaining historical buildings. In recent years, long–term vibration monitoring turned out to be an effective non-destructive technique to investigate the dynamic behaviour and check the health status of historical buildings. Changes in their dynamic properties, such as natural frequencies, can represent effective damage indicators. The latest NOSA-ITACA developments are oriented towards structural health monitoring. The availability of the experimental modal properties of a structure makes it possible to calibrate its finite element model via model updating procedures. In particular, the unknown structure's characteristics, such as materials' properties and boundary conditions, can be determined by solving a minimum problem whose objective function is expressed as the discrepancy between experimental frequencies and mode shapes

Maria Girardi
Institute of Information Science and Technologies "A. Faedo", ISTI–CNR, Pisa, Italy, e-mail: maria.girardi@isti.cnr.it

Cristina Padovani
Institute of Information Science and Technologies "A. Faedo", ISTI–CNR, Pisa, Italy, e-mail: cristina.padovani@isti.cnr.it

Daniele Pellegrini
Institute of Information Science and Technologies "A. Faedo", ISTI–CNR, Pisa, Italy, e-mail: daniele.pellegri@isti.cnr.it

Margherita Porcelli
Department of Mathematics, University of Bologna, Bologna, Italy - Institute of Information Science and Technologies "A. Faedo", ISTI–CNR, Pisa, Italy, e-mail: margherita.porcelli@unibo.it

Leonardo Robol
Department of Mathematics, University of Pisa, Pisa, Italy - Institute of Information Science and Technologies "A. Faedo", ISTI–CNR, Pisa, Italy, e-mail: leonardo.robol@unipi.it

and their numerical counterparts. Several case studies are presented to show the main features of NOSA-ITACA and its effectiveness in the conservation of architectural heritage.

1 Introduction

NOSA-ITACA is a finite element (FE) software package for the numerical modelling of the structural behaviour of heritage constructions. The free distribution of the code [6] is aimed at facilitating the use of mathematical models and numerical tools in the field of Cultural Heritage and draws its inspiration from the pioneering experiences of FEAP [29], Code–Aster [30] and Opensees [28] in the broader fields of computational thermomechanics and earthquake engineering.

The development of the code began in the 80s and has been made possible through the funding of the Italian National Research Council, the Italian Ministry of Universities and Research, and the region of Tuscany. In particular, within the framework of the NOSA-ITACA [20], [39] and MOSCARDO projects [22], the code has been substantially modified and significantly improved with the addition of new FORTRAN 90 modules, and equipped with new finite elements and functionalities, thus enhancing its application capabilities. NOSA-ITACA incorporates a FE numerical code (called NOSA, Nonlinear Structural Analysis), entirely developed by the Mechanics of Materials and Structures Laboratory of the ISTI-CNR (MMS Lab), relies on the open-source SALOME platform [31] for pre– and post–processing operations and enables static and dynamic analysis of structures made of linear elastic and masonry materials. The code adopts the constitutive equation of masonry-like materials [12], [13] and models masonry as a homogeneous isotropic nonlinear elastic material with zero or weak tensile strength and infinite or bounded compressive strength [35]. The package relies on a finite element formulation of the differential equations governing the statics of masonry structures. Suitable numerical techniques have been developed [35] based on the Newton–Raphson method for solving the nonlinear system obtained by discretizing the structure into finite elements. The code enables thermomechanical analysis of masonry-like solids in the presence of thermal loads [35] and can be applied to modelling restoration and reinforcement operations on constructions of architectural interest. Recent code applications to historical buildings can be found in [19] and [20].

Recently, numerical methods for constrained generalized eigenvalue problems have been implemented in NOSA-ITACA to address modal analysis of linear elastic structures [39]. The latest developments of the code focused on the integration of numerical simulations with experimental tests. Thus, algorithms for the finite element model updating, aimed at calibrating the FE model of a structure using its experimental frequencies and mode shapes have been implemented in NOSA-ITACA [22], along with a new numerical procedure, which relies on linear perturbation and allows to model the influence of cracks on the dynamical properties of a masonry structure [21].

This chapter describes the main features of the code and its effectiveness in the field of Cultural Heritage. Section 2 is devoted to a brief description of NOSA-ITACA and SALOME. A summary of the constitutive equation of masonry-like materials implemented in NOSA-ITACA is reported in Section 3. The nonlinear static analysis of masonry constructions and the modal analysis of linear elastic structures are addressed in Section 4. Two case studies modelled via NOSA-ITACA are reported for the sake of illustration: the static analysis of the church of San Francesco in Lucca and the modal analysis of the Devil's bridge in Borgo a Mozzano, in which the software is compared with some commercial codes in terms of reliability of results and computation time. Sections 5 and 6 are devoted to finite element model updating and linear perturbation and describe the algorithms recently implemented in NOSA-ITACA along with some applications.

2 The NOSA-ITACA code for the structural analysis of masonry buildings

NOSA-ITACA is free software developed by the MMS lab at ISTI-CNR. It is a finite element code that combines NOSA (the solver) with the open-source SALOME platform, suitably modified for pre– and post–processing operations. The current version of NOSA-ITACA enables conducting both linear and nonlinear static and modal analyses. The constitutive equations implemented in the code include isotropic linear elastic materials and masonry-like materials, modelled as nonlinear elastic materials with weak or zero tensile strength and infinite or bounded compressive strength. Several boundary conditions and load types can be prescribed, including multipoint constraints and thermal loads. The code contains an extensive element library, including beam, plane, shell, three-dimensional and axisymmetric elements [6].

The downloadable package NOSA-ITACA (www.nosaitaca.it/software/) includes SALOME v8.3.0, and is available for Ubuntu 16.04, 18.04 and 20.04 and works on any modern GNU/Linux system. It is possible to run NOSA-ITACA by simply downloading a compressed file and launching the executable. The solver NOSA, developed by MMS Lab, has been integrated into the open-source graphic software SALOME [31]. The NOSA-ITACA code resulting from the integration relies on SALOME to define the geometry of the structure under examination and visualize the results of the structural analysis. In particular, the integration implements the FE code NOSA (developed in Fortran) within the SALOME architecture (developed mainly in the C/C++ and Python languages) as an additional module like those already existing (MESH, GEOM, PARAVIS). The **SALOME Nosa** module allows the user to define the physical quantities associated to the mesh (materials, elements' thickness, boundary conditions, loads, type of analysis), display the load applied on the structure, generate the input file for running and monitoring the finite element analysis. The module includes a stand-alone version of the FE code as an executable file **nosao** and implements a GUI (Graphical User Interface) using Python and Qt 5

libraries. The GUI communicates with the SALOME kernel and additional modules (such as MESH) through CORBA interfaces, defined by IDL files. The executable **nosao** carries out the numerical analysis using as input the card "crd" created via the **SALOME Nosa** module. Moreover, the **SALOME Nosa** module allows the user to monitor the analysis and, finally, transmits the results of the numerical study to the visualization module PARAVIS by creating a "med" output file. Figure 1 shows a screenshot of a mode shape of the San Frediano bell tower in Lucca visualized by PARAVIS.

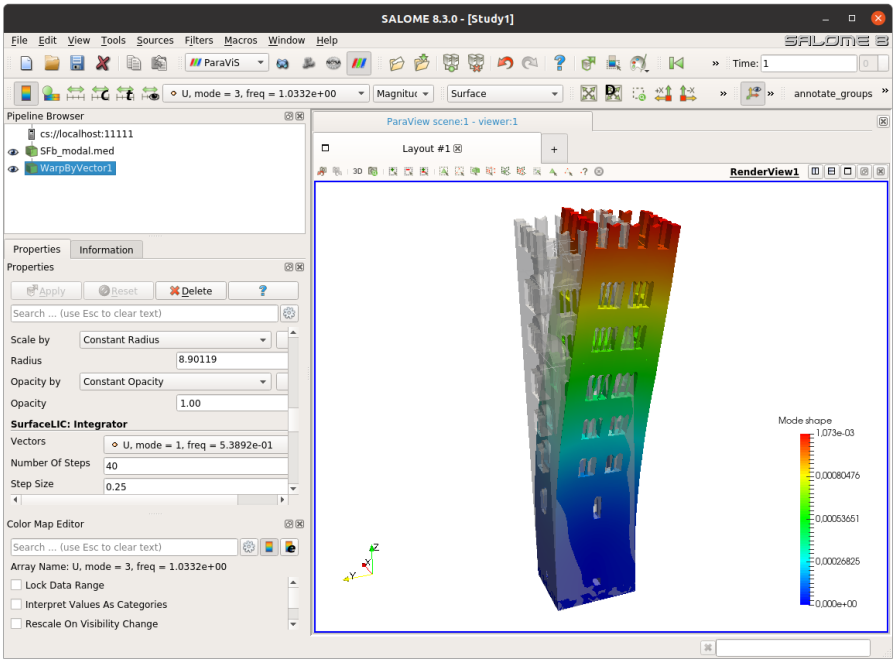

Fig. 1 PARAVIS module, visualization of a mode shape of the San Frediano bell tower.

3 The constitutive equation of masonry-like materials

Worldwide cultural heritage comprises different historical masonry constructions constituted by various materials such as stones, bricks, mortar, and built using different building techniques. Masonry materials share some common characteristics, the most relevant being that their response to tension is fundamentally different from compression, and their mechanical properties depend on the constituent elements and the construction techniques used. Among the constitutive equations available in the literature, NOSA-ITACA adopts the constitutive equation of masonry-like (or

no-tension) materials. This equation is inspired by the work of Heyman [27] on masonry arches and has been introduced and studied by Di Pasquale [13] and Del Piero [12].

The constitutive equation of masonry-like materials is based on three fundamental hypotheses: (i) Infinitesimal elasticity, (ii) A unilateral constraint on the stresses, which enforce the admissible stresses to belong to the cone of symmetric negative semidefinite tensors, (iii) An orthogonality condition between stress and fracture strain. This equation considers masonry as a homogeneous and isotropic nonlinear elastic material with zero tensile strength and infinite compressive strength and can realistically model the most significant aspects of masonry's behaviour.

Let Lin be the set of all second-order tensors with the inner product $\mathbf{A} \cdot \mathbf{B} = tr(\mathbf{A}^T\mathbf{B})$, $\mathbf{A}, \mathbf{B} \in Lin$, with $\mathbf{A}^T$ the transpose of $\mathbf{A}$. We denote by Sym the subspace of symmetric tensors and by Sym^- and Sym^+ the sets of all negative semidefinite and positive semidefinite elements of Sym. Let $\mathbb{C}$ be a positive definite symmetric fourth-order tensor from Sym to Sym satisfying

$$\mathbf{A} \cdot \mathbb{C}[\mathbf{B}] = \mathbf{B} \cdot \mathbb{C}[\mathbf{A}], \quad \text{for} \quad \mathbf{A}, \mathbf{B} \in Sym, \quad \mathbf{A} \cdot \mathbb{C}[\mathbf{A}] > 0 \quad \text{for} \quad \mathbf{A} \neq 0. \tag{1}$$

We can consider the inner product $\odot$ on Sym

$$\mathbf{A} \odot \mathbf{B} = \mathbf{A} \cdot \mathbb{C}^{-1}[\mathbf{B}], \quad \text{for} \quad \mathbf{A}, \mathbf{B} \in Sym, \tag{2}$$

and the associated norm $\| \mathbf{A} \|^2_{\mathbb{C}^{-1}} = \mathbf{A} \odot \mathbf{A}$. Given $\mathbf{E} \in Sym$ let us consider the functional

$$\psi(\mathbf{S}) = \| \mathbb{C}[\mathbf{E}] - \mathbf{S} \|^2_{\mathbb{C}^{-1}} = (\mathbb{C}[\mathbf{E}] - \mathbf{S}) \cdot (\mathbf{E} - \mathbb{C}^{-1}[\mathbf{S}]). \quad \mathbf{S} \in Sym^-. \tag{3}$$

The following proposition holds.

Proposition 1 *For $\mathbf{E} \in Sym$ there exists a unique $\mathbf{T} \in Sym^-$ satisfying the following three equivalent statements*

(i) $\mathbf{T}$ *minimizes functional* ψ

$$\psi(\mathbf{T}) \leq \psi(\mathbf{S}), \quad \text{for each} \quad \mathbf{S} \in Sym^-. \tag{4}$$

(ii) $\mathbf{T}$ *satisfies the variational inequality*

$$(\mathbb{C}[\mathbf{E}] - \mathbf{T}) \odot (\mathbf{S} - \mathbf{T}) \leq 0, \quad \forall \mathbf{S} \in Sym^-. \tag{5}$$

(iii) $\mathbf{T}$ *satisfies the following complementarity problem*

$$\mathbf{E} - \mathbb{C}^{-1}[\mathbf{T}] \in Sym^+, \quad \mathbf{T} \cdot (\mathbf{E} - \mathbb{C}^{-1}[\mathbf{T}]) = 0. \tag{6}$$

Sym^- is a convex closed cone of Sym, then the proposition follows from the minimum norm theorem [8] and $\mathbf{T}$ is the projection of $\mathbb{C}[\mathbf{E}]$ onto Sym^- with respect to the inner product $\odot$ in Sym

$$\mathbf{T} = P_{Sym^-}(\mathbb{C}[\mathbf{E}]). \tag{7}$$

Thus, given the elasticity tensor $\mathbb{C}$, which contains the mechanical properties of the material (as Young's modulus and Poisson's ratio), and the strain tensor $\mathbf{E} \in Sym$, the stress tensor $\mathbf{T}$ corresponding to $\mathbf{E}$ is the projection defined in (7). The strain $\mathbf{E}$ is the sum of an elastic part $\mathbb{C}^{-1}[\mathbf{T}]$, which depends linearly on $\mathbf{T}$, and an inelastic part $\mathbf{E} - \mathbb{C}^{-1}[\mathbf{T}]$, which belongs to the normal cone to Sym^- at $\mathbf{T}$ in virtue of (6). $\mathbf{E} - \mathbb{C}^{-1}[\mathbf{T}]$ is also called fracture strain because cracks are expected to be present in the regions in which it is different from zero. We can consider the stress function $\widehat{\mathbf{T}}$ from Sym to Sym^- defined by

$$\widehat{\mathbf{T}}(\mathbf{E}) = \mathbf{T}, \quad \text{with} \quad \mathbf{T} = P_{Sym^-}(\mathbb{C}[\mathbf{E}]).$$

The function $\widehat{\mathbf{T}}$ is non-linear, homogeneous of degree 1, monotone, Lipschitz continuous and Fréchet differentiable on a open dense subset of Sym [12], [35], [38].

If the elasticity tensor $\mathbb{C}$ is isotropic [26] then $\mathbb{C}[\mathbf{A}] = 2\mu\mathbf{A} + \lambda tr(\mathbf{A})\mathbf{I}$, where μ and λ are the Lamé moduli of the material satisfying the inequalities $\mu > 0$ and $2\mu + 3\lambda > 0$. In this case, by using the fact that $\mathbf{E}$, $\mathbf{T}$ and the fracture strain are coaxial, it is possible to calculate explicitly $\widehat{\mathbf{T}}(\mathbf{E})$ and its derivative $D_E\widehat{\mathbf{T}}(\mathbf{E})$, which is a symmetric positive semidefinite fourth-order tensor [35]. The latter will be used for the numerical solution of the static and dynamic problems of masonry structures.

It is well known that the mechanical behaviour of masonry constructions can be affected by thermal variations. A first contribution on the behaviour of masonry bridges subjected to thermal variations is given in [25], reporting on several masonry arch bridges that presented lowering of the crown during winter and rising during summer. More recent papers report the presence of cracks in masonry monuments and bridges, which can be ascribed to daily and seasonal thermal fluctuations [44], [7], [43]. Thus, to model the influence of temperature variations on the stress field, the crack distribution, and the dynamic properties of masonry structures, the constitutive equation of masonry-like materials can be generalized to consider the presence of thermal dilatation. So, we denote by θ the temperature, θ_0 the reference temperature, $\mathbb{C}(\theta)$ the elasticity tensor (the mechanical properties may depend on temperature), $\alpha(\theta - \theta_0)\mathbf{I}$ is the thermal expansion due to the thermal variation $\theta - \theta_0$, with α the coefficient of thermal expansion. As in the isothermal case, given the elasticity tensor $\mathbb{C}(\theta)$ and the infinitesimal strain tensor $\mathbf{E}$ and temperature θ, the stress tensor $\mathbf{T}$ corresponding to $\mathbf{E}$ and θ is the projection of $\mathbb{C}(\theta)[\mathbf{E} - \alpha(\theta - \theta_0)\mathbf{I}]$ onto Sym^- with respect to the scalar product $\odot$ in Sym defined by $\mathbb{C}(\theta)^{-1}$. The constitutive equation of masonry-like materials under non isothermal conditions has been implemented in NOSA-ITACA to model the behaviour of masonry buildings subjected to thermal loads [35].

4 Static and modal analysis

NOSA-ITACA relies on a finite element formulation of the partial differential equations governing the equilibrium of linear elastic and masonry buildings.

Let us consider a body[1] $\mathcal{B}$ whose boundary $\partial\mathcal{B}$ comprises two complementary and disjoined portions $\partial\mathcal{B}_1$ and $\partial\mathcal{B}_2$. $\mathcal{B}$ is made of a masonry-like material with constitutive equation (7). The equilibrium problem for a body $\mathcal{B}$ subjected to the loads ($\mathbf{b}$, $\mathbf{s_0}$), with the body force $\mathbf{b}$ defined over $\mathcal{B}$, and the surface force $\mathbf{s_0}$ defined over $\partial\mathcal{B}_2$, is to find a triple ($\mathbf{u}$, $\mathbf{E}$, $\mathbf{T}$) consisting of one vector and two tensor fields defined over $\mathcal{B}$, which satisfy the following equations[35]

$$div\mathbf{T} + \mathbf{b} = \mathbf{0}, \quad \mathbf{E} = \frac{\nabla\mathbf{u} + \nabla\mathbf{u}^T}{2}, \quad \mathbf{T} = \widehat{\mathbf{T}}(\mathbf{E}), \quad \text{on } \mathcal{B}, \tag{8}$$

$$\mathbf{u} = \mathbf{0} \quad \text{on } \partial\mathcal{B}_1, \quad \mathbf{Tn} = \mathbf{s_0} \quad \text{on } \partial\mathcal{B}_2. \tag{9}$$

The equilibrium problem (8)-(9) has been addressed in [2], [18], [35], [42], [34], where it is shown that the existence of a solution ($\mathbf{u}$, $\mathbf{E}$, $\mathbf{T}$) is not guaranteed for all load conditions. Moreover, if an equilibrium solution exists, it may not be unique in terms of displacements, and given two solutions, the corresponding stress fields coincide. In order to study real problems, the equilibrium problem of masonry structures can be solved via the finite element method. Suitable numerical techniques have been developed [35] based on the Newton-Raphson method for solving the nonlinear system obtained by discretizing the body $\mathcal{B}$ into finite elements. Their application is based on the explicit expression for $D_E\widetilde{\mathbf{T}}(\mathbf{E})$, which is needed to calculate the tangent stiffness matrix K_T. Thus, an iterative procedure has been implemented into the finite element code NOSA [35]. Given the hyperelasticity of masonry-like materials, the solution of the equilibrium problem does not depend on the choice of the loading process, at least in terms of stress. For numerical reasons, to avoid convergence problems, it is strongly recommended to assign the load incrementally. The linear algebraic system obtained at each iteration of each load increment is solved with a frontal solver [32], which does not require building the whole assembled system matrix. Since $D_E\widehat{\mathbf{T}}(\mathbf{E})$ is positive semidefinite, in order to avoid the occurrence of null pivot during the solution of the system, a regularization method is applied [37], and $D_E\widehat{\mathbf{T}}(\mathbf{E})$ is replaced by $\varepsilon\ \mathbb{C}$ at those Gauss points where it vanishes, with ε a suitably small real number.

Recently, numerical methods for generalized eigenvalue problems have been implemented in NOSA-ITACA to address the modal analysis of linear elastic structures. In particular, [39] describes the procedure implemented for solving the constrained generalized eigenvalue problem

$$K\,\mathbf{v} = \omega^2\,M\,\mathbf{v}, \quad T\mathbf{v} = 0, \tag{10}$$

where K and $M \in \mathbb{R}^{n\times n}$ and $T \in \mathbb{R}^{m\times n}$ with $m \ll n$. K and M are the stiffness and mass matrices of the finite element assemblage, K is symmetric and positive semidefinite, M is symmetric and positive definite, and both are banded with the bandwidth depending on the numbering of the finite element nodal points. The integer n is the total number of degrees of freedom of the system and is generally

[1] A body is a regular region of the three-dimensional Euclidean space having boundary $\partial\mathcal{B}$, with outward unit normal $\mathbf{n}$ [26].

very large since it depends on the discretization of the problem. The second condition in (10) expresses the fixed constraints and the master-slave relations assigned to the displacements of the structure. Restriction of the matrix K to the null subspace of $\mathbb{R}^n$ defined by T is positive definite. Solving (10) provides the natural frequencies $f_i = \omega_i/2\pi$ and mode shapes $\mathbf{v}^{(i)}$ of the structure. Algorithms implemented in NOSA-ITACA take into account both the sparsity of the matrices and the features of master-slave constraints (tying or multipoint constraints). They are based on the open-source packages SPARSKIT [41], for managing matrices in sparse format (storage, matrix-vector products), and ARPACK [33], which implements a method based on Lanczos factorization combined with spectral techniques that improve convergence. In order to make the code faster and able to compete with other state-of-the-art software, the inner solver of NOSA-ITACA has been paired with MUMPS [1], a direct sparse multi-frontal code both fast and well-tested by the numerical community.

4.1 The case study of the San Francesco Church

The results of some nonlinear structural analyses of the church of San Francesco in Lucca (Italy) are sketched to highlight the performance of NOSA-ITACA. The church is a typical single-nave Franciscan masonry building, about 70 m long, 16 m wide and 19 m high. The nave is closed on the west by the façade overlooking the San Francesco square (Fig.2) and on the east by the apse. The northern wall leans against the portico of the monastery cloister; the southern wall is instead completely free and runs along the street named via della Quarquonia. The earliest walls of the church date back to the 13th century, but the building underwent several changes and enlargements over the centuries [19]. The perimeter walls are mainly made of masonry bricks and lime mortar, except for the top of the longitudinal walls, where a band of poor quality masonry is present. At the end of the nineties, the southern wall presented large out-of-plane deflections and extensive cracks involving the masonry over the windows and near the facade. Some reinforcement operations, mainly aimed at improving the quality of the masonry and the connections between the walls, were concluded in July 2013. Because of the slenderness of the nave walls, it was decided to increase the building's resistance to horizontal actions. Thus, a metal framework was constructed at roof level to brace the structure, and the roof layer was stiffened through a crossed double-layer wooden deck. Numerical simulations were conducted via the NOSA-ITACA code to assess the effectiveness of the reinforcement operations [19] in light of current Italian regulations [15], [10], [14]. The church was subjected to the permanent and horizontal out-of-plane loads assigned incrementally and modelling equivalent static seismic actions. Figure 3 shows the fracture strain in the southern wall before (middle) and after (bottom) the strengthening intervention. The numerical results correspond to the fifth load increment (middle) and the seventh load increment (bottom), at which the church, respectively without and with reinforcement, reaches the life-safety ultimate limit

state. The fracture strain distribution calculated before the strengthening intervention matches the actual crack pattern (top), exhibiting vertical cracks between the façade and the lateral wall and over the windows. The figure highlights the benefits of the reinforcements, which reduced the values of both the fracture strain and the extension of the cracked region. In addition, the maximum value of the horizontal displacements, reached at the top of the longitudinal walls, is reduced by about 40% passing from the unreinforced to the reinforced case, while the maximum value of the compressive stress T_{zz} at the base of the church's walls, shown in Figure 4 vs. the total horizontal load H, is reduced by 30%. Therefore, the numerical analysis shows that applying the metal framework increases the church's resistance to horizontal actions and improves its global stability.

Fig. 2 Lucca, San Francesco square and the façade of San Francesco church.

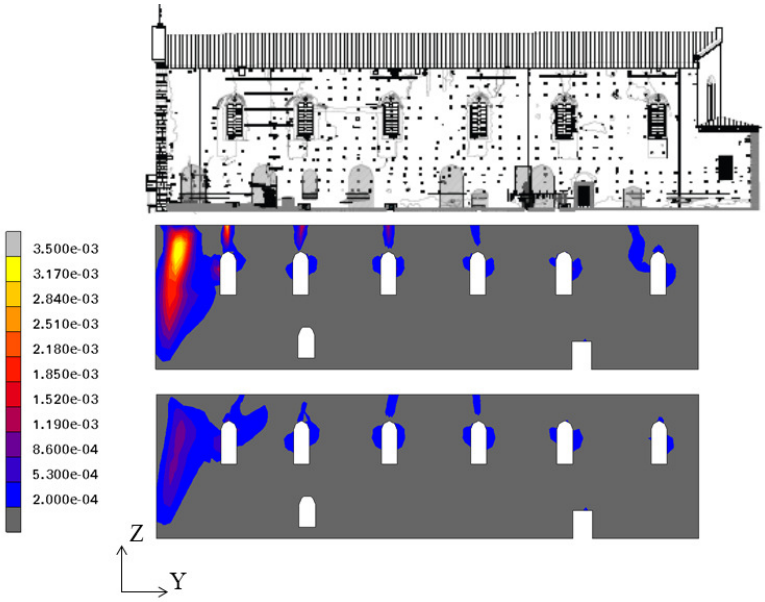

Fig. 3 San Francesco church: actual crack distribution in the southern wall before restoration (top), fracture strain before (middle) and after (bottom) restoration (equivalent static analysis).

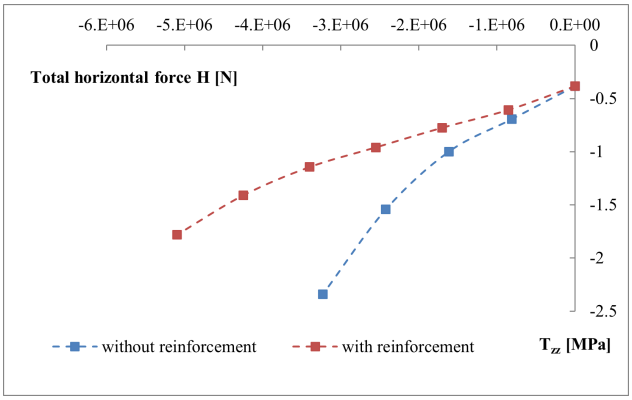

Fig. 4 Maximum values of compressive stress T_{zz} versus the horizontal load H applied to the church.

4.2 The case study of the Maddalena Bridge

In the following, a benchmark conducted on the case study of the Maddalena Bridge (Figure 5) in Borgo a Mozzano (Lucca) is described [3]. The bridge finite element model was analyzed via four different codes: NOSA-ITACA, Marc [36], SAP2000 (v14, [11]) and Code–Aster (v. LGPL 2016, [30]). The experiments, aimed at comparing the results of modal analysis, were performed on a server with an i7-920 CPU running at 2.67 GHz and 8GB of RAM. The performance of the four codes is compared in Table 1. The first ten natural frequencies evaluated by NOSA-ITACA and Marc are essentially coincident, and NOSA-ITACA, SAP2000 and Code–Aster yield very similar results. A comparison via the Modal Assurance Criterion (MAC) index [9] between the eigenvectors calculated with the different codes is also performed . The MAC values evaluated using the NOSA-ITACA eigenvectors and the eigenvectors calculated by the other codes all turn out to be greater than 0.98 (a MAC value near 1 indicates two almost parallel vectors). The experimental values of the natural frequencies are also available and reported in the last column of the table. Table 2 reports the computation times for the four codes. In terms of execution speed, Marc and Code–Aster outperform NOSA-ITACA, and SAP2000 turns out to be the slowest code. Table 2 also shows the number of degrees of freedom of the three models before and after the projection step (which in this context amounts to imposing the boundary conditions).

5 Ambient vibration test and finite element model updating

In order to assess the structural behaviour of historical monuments, numerical modelling can be integrated by experimental tests. In the ambient vibration tests, the vibrations induced by natural and anthropic sources (earthquakes, wind, traffic, crowd movements, et cetera) are recorded using a sensor network (accelerometers, velocimeters) installed on a historical building. Data recorded during the monitoring campaign are analyzed and processed using suitable numerical procedures that de-

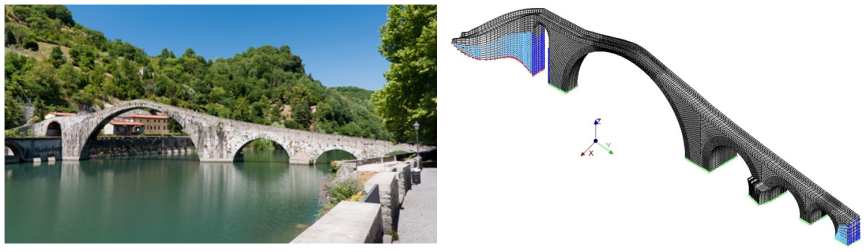

Fig. 5 The Maddalena bridge and its FE discretization.

Table 1 The Maddalena Bridge. Comparison between the frequencies computed by NOSA-ITACA (f_N), Marc 2013 (f_M), SAP2000 v14 (f_S) and Code–Aster v. LGPL 2016 (f_C), $d_{NM} = |f_N - f_M|/f_N$, $d_{NS} = |f_N - f_S|/f_N$, $d_{NC} = |f_N - f_C|/f_N$.

	$f_N\,[Hz]$	$f_M\,[Hz]$	$f_S\,[Hz]$	$f_C\,[Hz]$	$\delta_{NM}\,[\%]$	$\delta_{NS}\,[\%]$	$\delta_{NC}\,[\%]$	$f_{exp}\,[Hz]$
1	3.200	3.200	3.185	3.200	0.000	0.469	0.001	3.370
2	5.129	5.129	5.103	5.129	0.000	0.499	0.007	5.055
3	5.483	5.473	5.443	5.483	0.183	0.735	0.001	5.400
4	6.752	6.751	6.724	6.752	0.015	0.422	0.006	–
5	7.169	7.169	7.141	7.169	0.000	0.386	0.005	7.059
6	8.467	8.467	8.421	8.467	0.000	0.542	0.003	8.800
7	9.538	9.538	9.480	9.538	0.000	0.606	0.004	9.186
8	10.576	10.576	10.509	10.576	0.000	0.634	0.001	–
9	12.233	12.233	12.198	12.233	0.000	0.286	0.003	–
10	13.119	13.119	13.031	13.119	0.000	0.671	0.002	13.044

Table 2 Computation times for twenty of the smallest eigenvalues of the projected problem with NOSA-ITACA, Marc 2013, SAP2000 v14 and Code-Aster v. LGPL 2016, using the same Lanczos method accuracy settings. The number of degrees of freedom before and after the projection step are reported in the last two columns.

NOSA-ITACA	Marc	SAP2000	Code-Aster	No. DOF	No. proj. DOF
165.59 s	83.04 s	369.00 s	121.96 s	169,830	155,312

termine the structure's dynamic properties, such as frequencies, damping ratio and mode shapes. This approach is known as Operational Modal Analysis [9].

Using experimental modal properties of a structure makes it is possible to calibrate its finite element model via model updating procedures. The goal of finite element model updating is to determine the unknown characteristics of a structure, such as materials' properties, boundary conditions, et cetera by matching experimental and numerical frequencies and mode shapes [16].

We assume that the stiffness $K(\mathbf{x})$ and mass $M(\mathbf{x})$ matrices of the finite element model depend on a parameters vector $\mathbf{x}$ belonging to the box $\Omega \subset \mathbb{R}^p$, we solve the generalized eigenvalue problem (10) for $K(\mathbf{x})$ and $M(\mathbf{x})$ and we calculate the frequencies $f_1(\mathbf{x})$,... , $f_q(\mathbf{x})$ and the corresponding eigenvectors $\mathbf{v}_1(\mathbf{x})$,..., $\mathbf{v}_q(\mathbf{x})$. We consider the function

$$\phi(\mathbf{x}) = \sum_{i=1}^{q} w_i^2 [\hat{f}_i - f_i(\mathbf{x})]^2 + w_{q+i}^2 [1 - \gamma_i(\mathbf{x})]^2, \tag{11}$$

which measures the distance between the experimental frequencies $\hat{f}_i$ and mode shapes $\hat{\mathbf{v}}_i$ and the numerical counterparts $f_i(\mathbf{x})$ and $\mathbf{v}_i(\mathbf{x})$. Quantities $\gamma_i(\mathbf{x})$ are the absolute value of the cosine of the angle between the numerical and experimental mode shapes (the square root of the Modal Assurance Criterion defined in [9]). Scalars w_i are the weights that should be given to each frequency and mode shape in the optimization scheme (usually, $w_i = \hat{f}_i^{-1}$, for $i = 1, ..., q$ and $w_i = 0$ or $w_i = 0.1$ for $i = q+1, ..., 2q$). Then we minimize the objective function ϕ and we calculate a local

optimal value of $\mathbf{x}$ in Ω. The minimum problem we must solve is a nonlinear least square problem and the numerical procedure implemented in the NOSA-ITACA code to minimize function ϕ is based on a trust region scheme [22], [23]. By modifying the Lanczos's projection scheme used to compute the first (smallest) eigenvalues (and corresponding eigenvectors), we obtain local parametric reduced-order models that, embedded in the trust-region scheme, are the basis for an efficient algorithm that minimizes the objective function, starting from a point $\mathbf{x}_s$ belonging to Ω.

The model updating algorithm integrated within NOSA-ITACA reduces the overall computation time and can manage the large-scale problems encountered in the applications, where a large number of degrees of freedom are involved. It is worth noting that in many applications found in the literature, the finite element code (usually a commercial one) is used as a black-box function, and the optimization problem is solved using a general-purpose optimizer. The procedure implemented in NOSA-ITACA turned out to be faster than a black-box approach. Moreover, information about the reliability of the minimum point and its sensitivity to noisy experimental data can be obtained from the singular value decomposition of the Jacobian of the residual function (the difference between numerical and experimental frequencies) evaluated at the minimum point [23], [24].

To show the capabilities of the model updating procedure implemented in NOSA-ITACA, we consider the case study of the Clock Tower in Lucca shown in Figure 6. The tower dates back to the 13–th century [23], it is 48.4 m high, with a rectangular cross section of about 5.1 x 7.1 m and walls of a thickness varying from about 1.77 m at the base to 0.85 m at the top.

From November 2017 to March 2018 the ambient vibrations of the tower were monitored via four seismic stations adopting different layouts and four natural vibration frequencies and mode shapes were identified. The tower structure is discretized into 11,383 eight-node brick elements, the tie rods and wooden roofs are modelled using beam elements, for a total of 45,511 degrees of freedom. We assume that the structure is made of two different materials constituting the bell chamber (Material 1) and the tower (Material 2), respectively (figure 6). Poisson's ratio is fixed to 0.2, the mass densities are $\rho_1 = 1,700$ kg/m^3, $\rho_2 = 2,100$ kg/m^3 and the Young's moduli E_1 and E_2 are assumed to vary between 1 GPa and 6 GPa. For $\mathbf{x} = (E_1, E_2)$, the minimum point of function (11) calculated by NOSA-ITACA assuming $w_i = \hat{f}_i^{-1}$, $i = 1, ..., 4$, $w_5 = w_6 = 0.1$ and $w_7 = w_8 = 0$, has coordinates $E_1^{opt} = 1.9288$ GPa and $E_2^{opt} = 3.0451$. Figure 7 shows a plot of the objective function ϕ and Figure 8 shows the convergence of the numerical frequencies to the experimental ones during the process. Finally, Table 3 reports the experimental frequencies, the numerical frequencies calculated at the minimum point (E_1^{opt}, E_2^{opt}) and their relative errors. The total computation time was 27.15 s against 175.41 s required to minimize function ϕ with a general purpose optimizer (using the SQP solver of Matlab 2013b coupled with NOSA–ITACA as a black–box function).

Table 3 Results of the optimization algorithm: experimental and numerical frequencies and relative errors.

Mode Shape	Exp. freq. [Hz]	Num. freq. [Hz]	Relative error (%)
1	1.05	1.0440	0.57
2	1.30	1.31229	0.99
3	4.19	4.1884	0.04
4	4.50	4.4522	1.06

6 Structural health monitoring and linear perturbation

In recent years, continuous long-term vibration monitoring turned out to be an effective non-destructive technique to investigate the dynamic behaviour and check the health status of historical buildings. Long-term monitoring campaigns have shown that changes in the dynamic properties, such as natural frequencies and mode shapes, can represent effective damage indicators. In particular, experimental frequencies are sensitive to structural changes, but they also depend on environmental parameters, such as temperature and humidity. The long term dynamic monitoring of the San Frediano bell tower in Lucca reported in [4] has highlighted that frequencies tend to increase with temperature, with a variation during the year of 5-6 percent.

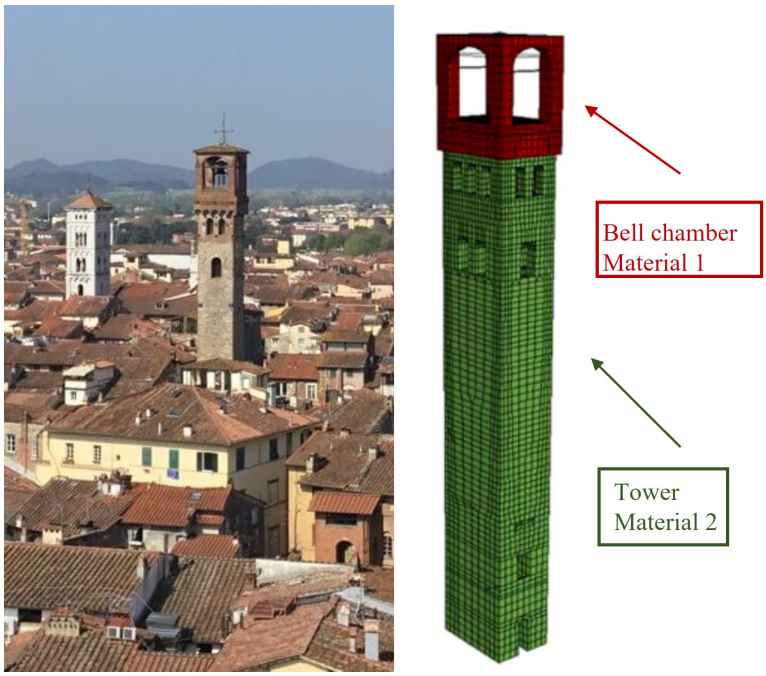

Fig. 6 The Clock Tower in Lucca (in the foreground on the left) and its finite element discretization (on the right).

This behaviour can be explained by the closure of cracks due to thermal dilatation in the materials constituting the tower, which tends to increase its stiffness. Once the influence of environmental factors has been considered, the changes in the dynamic properties over time can represent effective structural damage indicators, as shown in [17], reporting the results of a 15-month dynamic monitoring of the Gabbia tower in Mantova. During the monitoring period, the tower was subjected to a far-field seismic event, the Garfagnana earthquake in June 2013, characterized by a peak acceleration of about 20 cm/s^2, exceeding 40-50 times the highest amplitude of the usually observed ambient vibrations. The natural frequencies of the tower exhibit fluctuations induced by temperature and a sudden decrease of the modal frequencies on 21/06/2013, corresponding to the occurrence of the seismic event and associated to the damage in the tower after the Garfagnana earthquake.

The dependence of frequencies on structural changes is also highlighted in the paper [40], describing the results of some monitoring campaigns conducted on the Mogadouro clock tower in Portugal, dating back to the XVI century. Many deep cracks characterized the tower structure, that was therefore subjected to rehabilitation works in 2005, including the walls consolidation and the installation of tie-rods. To evaluate the structural response before and after rehabilitation, two ambient vibration tests were carried out. A comparison between the first seven frequencies of the tower before and after the consolidation works revealed a significant increase in the frequency values. Such results reflect the actual structural conditions of the tower, i.e. a lower-stiffness building with many cracks before rehabilitation and a higher-stiffness building after rehabilitation.

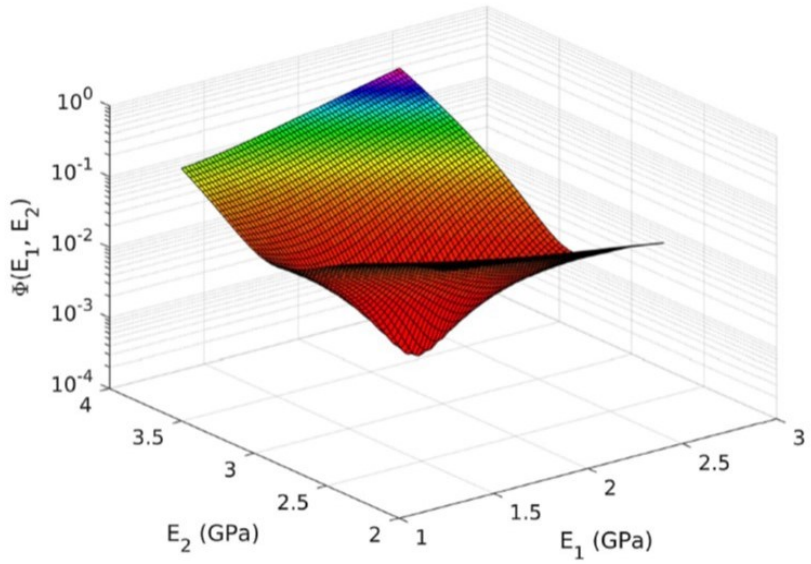

Fig. 7 Objective function ϕ vs. (E_1, E_2).

The latest NOSA-ITACA developments and applications are motivated by the above results and are oriented towards structural health monitoring. Our goal is to model the influence that both the nonlinear behaviour of the masonry material and the presence of cracked regions can have on the dynamic properties of masonry structures. The method implemented in NOSA-ITACA [21] is based on linear perturbation analysis, an approach adopted in mechanical and aerospace engineering to consider the effect of cracks on the vibration frequencies. Linear perturbation allows calculating the natural frequencies and mode shapes of masonry buildings in the presence of cracks. Given the structure under examination, discretized into finite elements, and given the mechanical properties of the constituent materials together with the kinematic constraints and loads acting on the structure, the procedure implemented in NOSA-ITACA consists of the following steps [21].

Step 1. The solution to the nonlinear equilibrium problem of the structure is calculated and the tangent stiffness matrix K_T to be used in the next step is evaluated.

Step 2. A modal analysis about the equilibrium solution is performed by using the tangent stiffness matrix K_T calculated in the last iteration of step 1, before the convergence is reached. The generalized eigenvalue problem (10) is then solved, with the tangent stiffness matrix K_T in place of the elastic stiffness matrix K.

The incremental approach used by NOSA-ITACA allows the user to perform modal analysis at the initial step (standard modal analysis considering the materials as linear elastic), before application of any load to the structure, and then for different loading steps, thus assessing the effects of the presence of cracks on the structure's dynamic properties. The new procedure provides for more realistic simulations of the dynamic behaviour of masonry structures [5] and, when combined with experimental

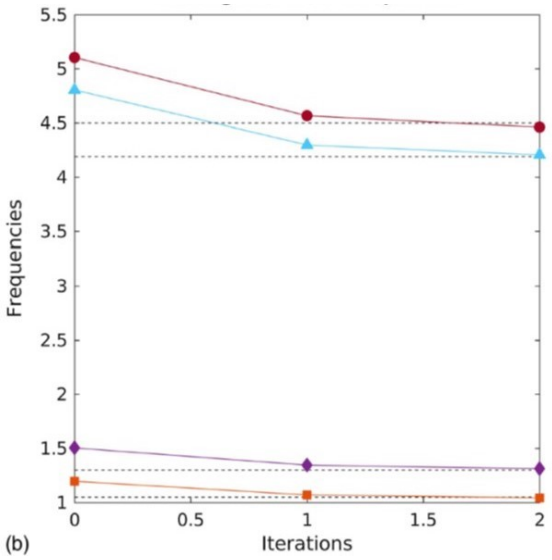

Fig. 8 Convergence history.

data, it can help in damage detection. Moreover, the dependence of the natural frequencies on external loads (both mechanical and thermal) can be assessed and used to interpret data from long-term monitoring campaigns.

In the following, we report the results of a linear perturbation analysis conducted on the San Frediano bell tower considering the temperature variations experimented by the tower during the monitoring period [4].

For each thermal load increment, the solution to the equilibrium problem is determined and the natural frequencies f_1 and f_2 are calculated. Figure 9 shows the correlation of the first two experimental frequencies with air temperature in Lucca's historic centre and describes the influence of temperature on the tower's modal properties.

As found in other long-term vibration monitoring campaigns on historical towers [17], frequencies tend to increase with temperature. This behaviour is confirmed from a numerical point of view by the trend of black squares in the figure, which represent the frequency values yielded by the nonlinear FE analysis of the tower subjected to incremental thermal variations.

The numerical simulation supports the hypothesis that an increase in temperature induces a reduction in the fracture strains within the masonry, thus increasing the structure's global stiffness. Similar behaviour is described in [25] for static loads, reporting closing/opening of cracks in bridges and vaults during the summer/winter.

7 Conclusions

This chapter describes the software NOSA-ITACA for the structural analysis of historical masonry constructions. NOSA-ITACA is the result of integrating NOSA, a FE code developed by the Mechanics of Materials and Structures Laboratory (MMS Lab) of ISTI-CNR, into the open-source graphical platform SALOME. The software adopts the constitutive equation of masonry-like materials, which models masonry as a homogeneous isotropic non-linear elastic material with zero or weak tensile strength and infinite or bounded compressive strength and enables static analysisis of structures made of linear elastic and masonry materials. NOSA-ITACA, whose first developments date back to the 80s, has been substantially modified in the last years, leading to a new release (NOSA-ITACA 1.1). Special attention has been given to modal analysis and model updating to support recent research activities of the MMS Lab, focused on the dynamic identification of ancient masonry buildings. These changes have contributed to making the performance of NOSA-ITACA comparable to state-of-the-art commercial software. NOSA-ITACA contains an extensive element library, including beam, plane, shell, three-dimensional and axisymmetric elements. In addition to perform static analyses under different loads and boundary conditions, also in the presence of thermal variations, NOSA-ITACA can be applied to modelling restoration and reinforcement operations on constructions of architectural interest. The latest developments of NOSA-ITACA are oriented to combine numerical simulations and structural health monitoring of historical buildings. Al-

gorithms for model updating and linear perturbation have been integrated into the package to calibrate finite element models using experimental data and assess the influence of damage on the dynamical properties of constructions.

The code is at the disposal of private and public bodies operating in the conservation and safeguarding of cultural heritage. The package is available at http://www.nosaitaca.it/software/ and works on any modern GNU/Linux system. It is now possible to run NOSA-ITACA 1.1 simply by downloading a compressed file and launching the executable.

The development of NOSA-ITACA is a work in progress, according to the research lines of the MMS Lab. Future work aims to expand the element library, generalize the constitutive model and introduce new algorithms for model updating.

Acknowledgements The development of NOSA-ITACA has been partially funded by the Region of Tuscany within the framework of projects NOSA-ITACA (PAR- FAS 2011-2013) and MOSCARDO (FAR-FAS 2016-2018). This financial support is gratefully acknowledged.

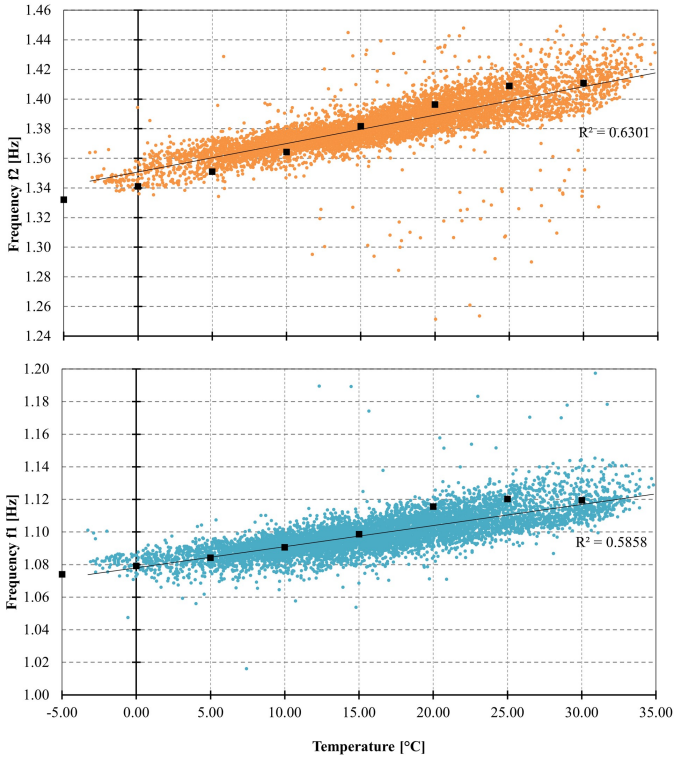

Fig. 9 The San Frediano bell tower, first and second natural frequency vs temperature.

References

1. Amestoy, P.R., Duff, I.S., L'Excellent, J.Y., Koster, J.: MUMPS: a general purpose distributed memory sparse solver. Lecture Notes in Computer Science, 121–130 (2001)
2. Anzellotti, G.: A class of convex non-coercive functionals and masonry-like materials. Annales de l'Institut Henri Poincaré C, Analyse non linéaire **2(4)**, 261–307 (1985)
3. Azzara, R.M., De Falco, A., Girardi, M., Pellegrini, D.: Ambient vibration recording on the Maddalena Bridge in Borgo a Mozzano (Italy): data analysis. Annals of Geophysics **60(4)** (2017)
4. Azzara, R. M., De Roeck, G. , Girardi, M., Padovani, C., Pellegrini, D., Reynders, E.: The influence of environmental parameters on the dynamic behaviour of the San Frediano bell tower in Lucca. Engineering Structures **156**, 175-187 (2018)
5. Azzara, R.M., Girardi, M., Padovani, C., Pellegrini, D.: Experimental and numerical investigations on the seismic behaviour of the San Frediano bell tower. Annals of Geophysics **62(3)**, SE342 (2019)
6. Binante, V., Girardi, M., Padovani, C., Pasquinelli, G., Pellegrini, D., Porcelli, M., Robol, L.: NOSA-ITACA 1.1 documentation 2017. http://www.nosaitaca.it
7. Blasi, C. , Coisson, E.: The effects of temperature on historical stone masonry structures. Structural Analysis of Historic Construction: Preserving Safety and Significance, 1271–1276 (2008).
8. Brezis H.: Analyse fonctionnelle - theorie et applications. Masson Editeur, Paris (1983)
9. Brincker R, Ventura C.: Introduction to Operational Modal Analysis. John Wiley & Sons (2015)
10. Circolare 2 febbraio 2009, n. 617, C.S.LL.PP, Istruzioni per l'applicazione delle nuove norme tecniche per le costruzioni di cui al D.M: 14 gennaio 2008.
11. CSI Analysis Reference Manual For SAP2000®. ETABS, SAFE and CSiBridge, Berkeley, California, USA, December 2011.
12. Del Piero, G.: Constitutive equations and compatibility of external loads for linear elastic masonry–like materials. Meccanica **24**, 150–162 (1989)
13. Di Pasquale, S.: New trends in the analysis of masonry structures. Meccanica **27**, 173–184 (1992)
14. Direttiva del Presidente del Consiglio dei Ministri del 9 febbraio 2011: Valutazione e riduzione del rischio sismico del patrimonio culturale con riferimento alle Norme Tecniche per le Costruzioni di cui al D. M. 14 gennaio 2008. G.U. n. 47 del 26 febbraio 2011 - Suppl. ord. N. 54.
15. D.M. 14 gennaio 2008, Norme Tecniche per le Costruzioni, G.U. 4 febbraio 2008, n. 29.
16. Friswell, M., Mottershead, J.E.: Finite element model updating in structural dynamics. Springer Science and Business Media **38** (2013)
17. Gentile, C., Guidobaldi, M., Saisi, A.: One-year dynamic monitoring of a historic tower: damage detection under changing environment. Meccanica **51(11)**, 2873-2889 (2016)
18. Giaquinta, M., Giusti, E.: Researches on the equilibrium of masonry structures. Archive for Rational Mechanics and Analysis **88(4)**, 359-392 (1985)
19. Girardi, M., Padovani, C., Pasquinelli, G.: Numerical modelling of the static and seismic behaviour of historical buildings: the church of San Francesco in Lucca. In: B.H.V. Topping, P. Ivanyi (eds.) Proceedings of CC2013 - Fourteenth International Conference on Civil, Structural and Environmental Engineering Computing article n. 80 (2013).
20. Girardi, M., Padovani, C., Pellegrini, D.: The NOSA-ITACA code for the safety assessment of ancient constructions: a case study in Livorno. Advances in Engineering Software **89**: 64–76 (2015)
21. Girardi, M. Padovani, C., Pellegrini, D.: Modal analysis of masonry structures. Mathematics and Mechanics of Solids **24(3)**, 616-636 (2019)
22. Girardi, M., Padovani, C., Pellegrini, D., Porcelli, M. Robol, L.: Finite element model updating for structural applications. Journal of Computational and Applied Mathematics **370**, 112675 (2018)

23. Girardi, M., Padovani, C., Pellegrini, D. Robol, L.: Model updating procedure to enhance structural analysis in FE code NOSA-ITACA. Journal of Performance of Constructed Facilities **33(4)**, DOI: 10.1061/(ASCE)CF.1943-5509.0001303 (2019)
24. Girardi, M., Padovani, C., Pellegrini, D., Robol, L.: A finite element model updating method based on global optimization. Mechanical Systems and Signal Processing **152**, 107372 (2021)
25. Guidi, C.: Influenza della temperatura sulle costruzioni murarie. Atti della Reale Accademia delle Scienze di Torino, 319–330 (1906)
26. Gurtin ME.: The linear theory of elasticity. In: Truesdell C. (Ed) Encyclopedia of Physics, Vol. VIa/2, Mechanics of Solids II, Springer-Verlag (1972)
27. Heyman, J.: The stone skeleton. International Journal of solids and structures **2**(2), 249–279 (1966)
28. http://opensees.berkeley.edu/
29. http://projects.ce.berkeley.edu/feap/
30. https://www.code-aster.org
31. http://www.salome-platform.org
32. Irons, B.M.: A frontal solution program for finite element analysis. International Journal for Numerical Methods in Engineering **2(1)**, 5–32 (1970)
33. R. B. Lehoucq , D. C. Sorensen, C. Yang, ARPACK Users Guide. Solution of Large Scale Eigenvalue Problem with Implicit Restarted Arnoldi Methods, SIAM, 1998.
34. Lucchesi, M.: A numerical method for solving BVP of masonry-like solids. In: M. Angelillo (ed.) Mechanics of Masonry Structures, International Centre for Mechanical Sciences Courses and Lectures **551**, 71–104 (2014)
35. Lucchesi, M., Padovani, C., Pasquinelli, G., Zani, N.: Masonry constructions: mechanical models and numerical applications. Lecture Notes in Applied and Computational Mechanics Springer–Verlag (2008)
36. Marc 2014 Volume A: theory and user information. Marc and Mentat, 2014, Marc and Mentat Docs.
37. Nocedal, J., Wright, S.J.: Numerical optimization. Springer, New York (2006)
38. Padovani C., Silhavy M.: On the derivative of the stress-strain relation in a no-tension material. Mathematics and Mechanics of Solids **22(7)**, 1606–1618 (2017)
39. Porcelli, M., Binante, V., Girardi, M., Padovani, C., Pasquinelli, G.: A solution procedure for constrained eigenvalue problems and its application within the structural finite-element code NOSA–ITACA. Calcolo **52(2)**, 167–186 (2015)
40. Ramos, L.F., Marques, L., Lourenço, P.B., De Roeck, G., Campos-Costa, A., Roque, J.: Monitoring historical masonry structures with operational modal analysis: two case studies. Mechanical systems and signal processing **24(5))**, 1291-1305 (2010)
41. Saad, Y.: Iterative methods for sparse linear systems. SIAM (2003)
42. Silhavy, M. : Mathematics of the masonry-like model and limit analysis. In: M. Angelillo (ed.) Mechanics of Masonry Structures, International Centre for Mechanical Sciences Courses and Lectures **551**, 29–69 (2014)
43. Talebinejad, I., Fischer, I., Ansari, F.: A hybrid approach for safety assessment of the double span masonry vaults of the Brooklyn Bridge. Journal of Civil Structural Health Monitoring **1(1-2)** 3–15, (2011)
44. Taliercio, A., Binda, L.: The Basilica of San Vitale in Ravenna: Investigation on the current structural faults and their mid-term evolution. Journal of Cultural Heritage **8**, 99–118 (2008)